Numerical model for solar thermal collectors and thermal energy storages based on phase change slurry

Numerical Model for Solar Thermal Collectors and Thermal Energy Storages Based on Phase Change Slurry

Gaia Prearo, Gianluca Serale and Marco Perino

Politecnico di Torino, DENERG Energy Department, Turin (Italy)

Abstract

The efficiency of conventional solar thermal collectors and related thermal energy storages is often reduced by the requirement for high irradiation levels and the heat losses due to the relatively high temperature of the heat transfer fluid. In order to overcome those limitations, a solar thermal system capable of working at low temperatures through the exploitation of latent heat storage is presented in this paper. The proposed system was based on a novel heat transfer fluid and storage media, composed by a mixture of water and micro-encapsulated phase change material (PCM), named Phase Change Slurry (PCS). This paper introduces a numerical model capable of accurately describe the physical process and the dynamics of the proposed technology (collector, thermal energy storage and control logics). Results were validated by means of experimental tests and a long-term monitoring on a real full-scale prototype. Furthermore, experimental tests were performed to carry out the actual PCS thermo-dynamical properties that are strongly dependent on the concentration of micro-capsules in the heat transfer fluid.

Keywords: Phase Change Material (PCM), HVAC system, solar thermal system, Phase Change Slurry (PCS), Latent Heat Thermal Energy Storage (LHTES),

1. Introduction

The pursuit to obtain higher levels of comfort has led to a dramatic increase of the energy demand in buildings. In Europe the overall energy demand of the building sector accounts for about 40 % of the total energy consumption (Pérez-Lombard et al., 2008). Solar technologies are a leading solution to face the challenge of reducing the impact of the building sector (http://www.iea-shc.org/programme-description). However, the full profitability of RES is often limited to a great extent by their stochastic variation and the time mismatch between availability and demand (Heier et al., 2015). Thus, energy storage strategies are becoming a crucial requirement to partially mitigate this gap.

A field that is particularly promising is represented by active Thermal Energy Storage (TES) technologies, (SHC Annual Report, 2012). Indeed, in buildings the active TESs allow the surplus of energy production to be stored and then released whenever demanded by the occupant. In particular, the peak power consumption can be mitigated by means the adoption of the TES. In this way the RES are better exploited and the size of the auxiliary systems can be effectively reduced. For the implementation of storage technologies directly into the buildings, compact tank solutions are required.

A further improvement in TES performance has been represented by the introduction of solutions exploiting latent heat exchanges. These solutions are commonly referred as Latent Heat Thermal Energy Storages (LHTES) and can be based on different technologies and storage media (e.g.: ice cold storages, salt hydrates, Phase Change Materials). Advances in industrial technologies have led to the development of Phase Change Materials (PCM), whose phase transition process occurs in many temperature ranges. Thus it is possible to select the material whose features are the most suitable for each specific application. The exploitation of latent heat represents a possible benefit in terms of reducing the size of the component and improving the overall system performance (Rodriguez-Ubinas et al., 2012). Indeed, on one hand the great amount of energy due to the phase change increases the energy stored density. On the other hand, the phase change can be exploited to reduce the temperature differences affecting the system, thus improving the overall system performance by

doi:10.18086/swc.2017.31.12 Available at http://proceedings.ises.org

means of a reduction of both the dispersion and the internal entropy dissipations.

Nowadays, the scientific literature offers numerous works dealing with technologies and solutions concerning LHTES. Particularly encouraging are those in which LHTES is coupled with solar thermal systems. In general, the presence of a PCM leads to an overall annual increase in the solar fraction, a higher efficiency of the system and major storage heat capacity. In the last few years, the use of PCMs has been tested in several different types of solar thermal systems. Three different methods in particular have been proposed to incorporate PCMs into solar thermal systems: the integration of a PCM directly in a layer of the solar collector (Sharma and Chen, 2009 and Eames and Griffiths, 2006), the addition of PCM nodes to the primary HTF solar loop pipes (Haillot et al., 2013) and the addition of PCM elements to the inside of a storage tank (Cabeza et al., 2006).

In 2015, some of the authors of the present paper (Serale et al., 2015) proposed an innovative solar thermal system based on Phase Change Slurry (PCS). The PCS is a mixture of water with glycol and a dispersed micro-encapsulated Phase Change Material (PCM). Micro-capsules allow the PCS to be pumpable regardless the state of aggregation of the material contained in their core. For this reason, it was possible to use the PCS both as the storage media and the Heat Transfer Fluid (HTF) in the primary loop of the solar thermal system. In this way, the phase change transition occurred also in the collector reducing the operating temperatures of the system due to the exploitation of latent heat exchange instead of a traditional sensible HTF temperature increasing. On the one hand the system dispersions to the ambient were reduced and on the other hand the fraction of hours of exploitable solar radiation were also increased, due to a reduction of the threshold limit of the solar radiation necessary to produce energy.

In order to investigate the potentialities of this PCS-based technology, a numerical model for solar thermal collector based on latent heat exchanged was formulated extending the Hottler-Willier for traditional solar thermal collectors (Serale et al., 2016). The present paper is an extension of the numerical model formulated in (Serale et al., 2016). In particular, the extended model herewith presented considers not only the collector, but the entire solar thermal system, including also the system PID controller and the LHTES tank. The integration of these models with the one previously built of the solar thermal collector, allowed a simulation of the prototype as a whole. Eventually, the paper shows the validation process of the numerical model using data gathered during an experimental campaign and a field test on a real-scale prototype.

The work is organised as follow. Section 2 summarises the main features of the numerical model of the collector, the TES and the closed-loop controller for solar thermal system capable of exploiting both latent and sensible heat. Section 3 briefly introduces and describes the solar thermal system analysed as case study. Section 4 reports the results of the experimental tests necessary to characterise the PCS used as HTF. Section 5 outlines the results of an experimental campaign undertaken to validate the numerical model with real data gathered on field. Section 6 is the conclusion of the work.

2. Methods: a numerical model for solar thermal systems exchanging latent heat and sensible heat

In order to better investigate the opportunities offered by the adoption of PCS in solar thermal system, a numerical model was necessary to perform simulation and parametrical analysis. These allow the system performance to be tested under different boundary conditions and climatic parameters. The numerical model had to be capable to describe both the sensible and the latent heat exchanges occurring in the system. In this way both traditional water-based and innovative PCS-based HTF can be tested and the system performance compared. The following Figure 1 provides a comprehensive framework of the numerical model carried out in the present work.

The solar thermal system model was characterised by 3 key elements: the collector model, the TES model and the closed loop controller that regulates the pump speed, thus the flow rate flowing in the system. Both the collector model and the TES model were finite elements thermodynamic models capable to describe the system evolution in terms of internal energy and temperature of the nodes. The model was entirely developed by means of Matlab scripts and Simulink flows. The model can be used to simulate both traditional water-based and PCS-based solar thermal systems. The switch between the two options can be uptaken by different setting of the features of the heat transfer fluid and storage media. Since the numerical model has to work both with water and with a phase change material, an enthalpy approach, instead of a temperature one, was used to

evaluate the internal energy of the system. In this way it was exploited the property of the enthalpy itself of being a continuous and invertible function of the temperature ($h=h(T)$).

The external disturbances influencing the system were the external weather conditions and the energy demand by the occupants. The external weather conditions that mainly affect the system heat exchanges were the ambient temperature T_a, the beam solar radiation G_b, the diffuse solar radiation G_d, the angle of incidence of the solar radiation θ on the collector, the wind velocity w_a, and the radiative temperature of the sky T_{sky}. The TES model considered the ambient temperature as unique weather disturbance, while the solar thermal collector model was affected by all the previous parameters. The occupancy energy demand affected the model of the TES and in particular the inlet temperature of the heat exchanger $T_{hx,in}$ and the thermal energy required in the heat exchanger Q_{hx}. Some general assumptions and simplifications were made in the model to make the physical–mathematical description of the components easier:

- quasi steady-state of the collector components (cover, plate, back insulation casing);
- uniform weather boundary conditions over all the system components;
- heat loss toward the same heat sink, considered at the outdoor air temperature;
- the HTF has constant density and thermal conductivity;
- the temperature of the HTF in the outlet of the collector is, unless a negligible error, the temperature in the inlet of the TES.
- the temperature in the outlet of the TES is approximately equal to the inlet temperature of the solar collector.

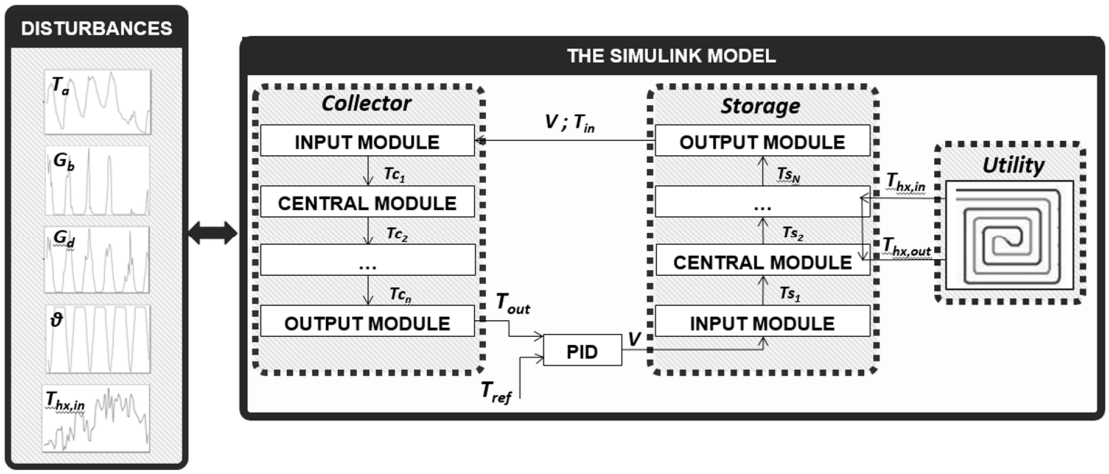

Fig. 1: General framework of the numerical model for solar thermal systems exchanging latent and sensible heat.

2.1 Numerical model for solar thermal collectors based on sensible or latent Heat Transfer Fluids

The solar thermal collector numerical model is the evolution of the previous version presented in (Serale et al., 2016). The numerical model was suitable to simulate different type of HTFs, thus with different thermo-physical properties. In this new version of the numerical model, the collector was a-priori discretised in 10 segments of the same length. Each segment was a lumped node having constant thermodynamic properties (e.g., temperature, specific enthalpy, conductivity, etc.). For each segment an energy balance based on the Hottel-Willier model for solar thermal collector was formulated and computed in order to carry out the temperatures of the components and the heat fluxes involved in the process (Duffie & Beckman, 2013). The solution of this energy balance depended on the HTF used, thus the thermal and rheological proprieties of the HTF had to be set in the model as a function of its temperature. In particular, the adoption of specific enthalpy vs. temperature curves defined by means of look-up tables allowed the model to be easily switchable from sensible to latent heat exchanges.

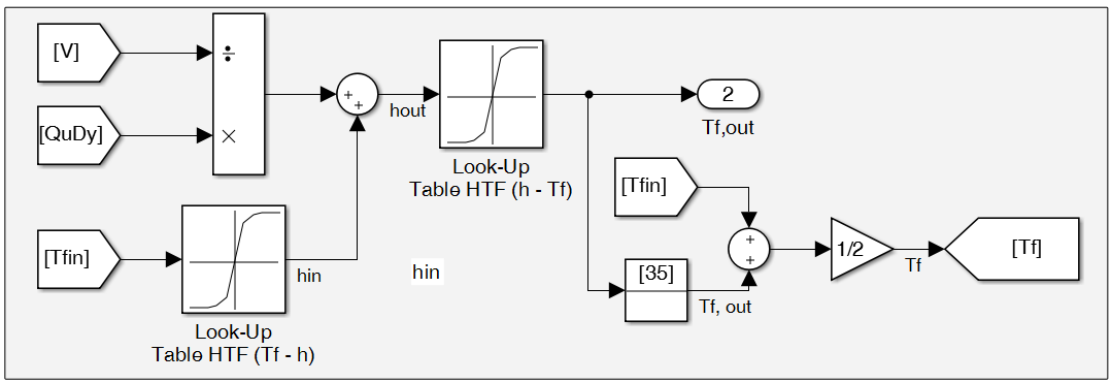

Fig. 2: The sub-section of the Simulink model exploiting the look-up tables used to define the HTF temperature as a function of the enthalpy.

2.2 The multi-node Thermal Energy Storage numerical model

A dynamic lumped energetic model was used to reproduce the thermal behaviour of the TES. In particular, a multi-node model (Streicher, 2008) was selected as the most suitable one to simulate with good accuracy the TES filled either with water or with PCS. Consequently, the TES tank has been virtually segmented into 7 lumped nodes representing finite horizontal volumes. Each node was considered filled with the internal storage media perfectly mixed, thus at one uniform temperature. Likewise the collector model, every node is influenced only by the flow rate entering from the previous one and it influences only the subsequent. The initial node receives the outlet flow rate of the collector, while the terminal node determines the inlet flow rate of the collector.

For each TES node the energy balance was defined by means of Eq.1.

$$\dot{Q}_{dp,j} + \dot{Q}_{hx,j} + \dot{Q}_{aux,j} + \dot{Q}_{cond,j} + \dot{Q}_{loss,j} = m_j \cdot \frac{h_j^{n+1} - h_j^n}{dt} \qquad \text{(eq.1)}$$

This balance considered negligible the pressure drop inside the tank and the heat losses to the ambient were taken into account using a global heat transfer coefficient. Referring to each j-th node of mass m, $\dot{Q}_{dp}$ is the heat flux due to the mass flow rate coming from the solar collector, $\dot{Q}_{hx}$ is the heat flux exchanged with the heat exchanger that delivers the space heating energy, $\dot{Q}_{aux}$ is the heat provided by an auxiliary heating source (e.g., a backup boiler or a backup electric heater), $\dot{Q}_{cond}$ is the heat flux exchanged by conduction between two adjacent nodes and $\dot{Q}_{loss}$ is the energy losses to the outdoor environment. The adoption of specific enthalpies h discretised over time on the right term of eq. 1 allowed the TES model to be easily adapted to the HTF used as storage media by means of the same temperature dependent look-up tables adopted for the model of the collector.

During an experimental campaign, every term of eq. 1 for each *j*-th node could be easily derived from the data gathered by thermocouples suitably placed into the TES. If the thermocouples in the TES were not enough to enable the direct solution of the balance in each node (e.g., temperatures monitored in the TES inlet and outlet only), the intermediate node temperatures would be linearly interpolated from these terminal data. Indeed, a quasi-linear trend could be justified by the very small temperature difference between the inlet and the outlet (e.g., at most 10 °C).

2.3 The control loop in the numerical model

Coping with a phase change fluid, the control logic was more complicated compared to traditional water based solar thermal systems. On one side, the controller had to avoid the overcoming of some technology limits of the system components (e.g., not exceed the 60°C maximum temperature thresholds that can damage the system). These control logics for the PCS-based solar thermal system could be based on Rule Based Controllers (RBC) extensively discussed in (Serale et al., 2015).

On the other side, an effective control logic was essential to fully exploit the available solar radiation and to optimise the coupling of the production with the users' demand. In order to maximise the overall energy

efficiency of the system the HTF latent heat should be exploited as much as possible. For this reason, the optimal working condition of the solar collector could be approximated to the one in which the PCS concludes its transition phase (around 40 °C) exactly at the collector outlet. In this way the heat for the isothermal phase change could be fully exploited and the thermal losses can be minimised by maintaining the lowest possible average working temperature of the solar panel. This control logic was addressed by means of a PID controller that managed the primary collector loop pump speed, thus the HTF flow rate flowing in the solar thermal collector. The target of the PID was to maintain the collector outlet temperature as much closer as possible to the set-point equal to the end of PCM transition phase.
The PID controller was implemented in the numerical model to control the flow rate flowing between the solar thermal collector and the TES tank. In the case of PCS the collector outlet temperature, which is the PID set-point, was set equal to 40 °C, a temperature slightly above the upper limit of the material phase change transition and always sufficient to guarantee the supply temperature for space heating. This allows the latent heat of the PCM to be fully exploited. The parameters of the PID controller were changed in the simulation model to evaluate the dynamic response of the system, and to tune the real controller of the prototype. Whereas the P value allows to reach the set-point faster, the I value deletes the error in regime permanent when the disturbances are constants and the D value allows to anticipate the future trend of the error. After preliminary tests, the controller was simplified to a Proportional-Integral controller and the Derivative term was neglected. Indeed, in this specific application, the disturbances - such as the solar radiation and the ambient temperature - are extremely variable, thus predicting the future error would also increase the instability of the system.

2.4 Auxiliary equations for considering the Phase Change Slurry features

A numerical model for a PCS-based solar thermal system required the proper setting of the PCS thermo-physical and rheological properties. These properties strongly depended on the concentration of the micro-encapsulated PCM in the PCS mixture. However, whereas the thermal properties could be easily calculated as the mass weighted average of the properties of the two components of the slurry, the rheological features showed a highly non-linear behaviour. Thus, the choice of the concentration of micro-encapsulated PCM dispersed in the mixture was not trivial. Indeed, it affected both the energy required in pumping and heat transfer, thus in the efficiency and in the energy savings of the system in real building applications. The selection of the most suitable concentration was a quite tricky trade-off, since enhancing a characteristic may cause the worsening of the other one. Indeed, boosting the concentration of micro-encapsulated PCM increased the available latent energy stored in the PCS mixture, but at the same time it determined higher pressure drops due to the increased fluid viscosity, which in turn means higher energy demand for pumping. However, higher thermal storage capacity also implied lower flow rate, and thus a reduction in electric energy demand from the pump (Serale et al., 2014). For these reasons, the authors decided to develop the model with PCS thermal and rheological characteristics that varies accordingly to the micro-encapsulated PCM concentration in the mixture, defined as φ. PCS viscosity and thermal conductivity were defined by means the following eq.2, eq.3 and eq.4, while the enthalpy or specific heat vs. temperature curves were determined with experimental tests for different concentrations.
On the one hand, the PCS dynamic viscosity has been calculated taking advantage from the Vand's model (eq 2):

$$\frac{\eta_b}{\eta_f} = (1 - \varphi - A\varphi^2)^{-2,5} \qquad \text{(eq.2)}$$

where η_b is the dynamic viscosity of the micro-encapsulated PCM, η_f is the dynamic viscosity of the dispersing phase, thus the water with concentration, φ is the volumetric concentration of the micro-encapsulated PCM in the mixture and A is a constant value that depends on the diameter and the geometry of the micro-capsule.
On the other hand, the PCS thermal conductivity was estimated by means of the (eq.3 and eq.4):

$$\frac{\lambda_{eff}}{\lambda_b} = 1 + B\ \varphi\ Pe_p^m \qquad \text{(eq.3)}$$

$$\frac{\lambda_b}{\lambda_f} = \frac{\left(2+\frac{\lambda_p}{\lambda_f}+2\varphi\left(\frac{\lambda_p}{\lambda_f}-1\right)\right)}{\left(2+\frac{\lambda_p}{\lambda_f}-\varphi\left(\frac{\lambda_p}{\lambda_f}-1\right)\right)} \qquad \text{(eq.4)}$$

where λ_{eff} is the thermal conductivity for the flowing PCS fluid, λ_b is the conductivity of the PCS in static conditions, λ_f is the conductivity of the fluid in which the micro-encapsulated PCM is dispersed, whereas Pe_p is the Péclet number of the particle. This last parameter depends on the dimension of the particle and of the pipe in which the fluid flows, on the radial position of the particle in the pipe and, moreover, on the mean velocity of the fluid. Finally, B and m can be considered as constants for defined ranges of the Péclet number.

3. Materials: a PCS-based solar thermal system

In order to validate the model, a real-scale prototype was necessary to undertake an experimental campaign and gather monitored data. In particular, the solar thermal collector and TES prototype described in (Serale et al., 2015) was used to this purpose. This prototype was designed to couple well with low temperature space heating terminals (e.g. radiant panels or Thermal Activated Building Elements). The prototype can use as HTF and storage media either water, eventually with glycol, or a PCS, which exploits the latent heat. The TES was powered by a flat plate solar thermal collector and heat was delivered to the building through a secondary heat exchanger placed inside the component. Furthermore, a complete monitoring system was installed in the prototype to gather data every second about the temperatures and the flow rates of the various components. In particular, energy meters monitored the electrical consumption of the auxiliaries, 20 thermocouples were placed in the collector, in the TES and in some crucial points of the pipes, 2 manometers (one for each loop) and a Corioli's flow meter were used in the secondary loop to measure the fluid flow rate inside the heat exchanger of the TES. On one side of the collector, a pyranometer measures the global solar radiation on the collector tilted plane.

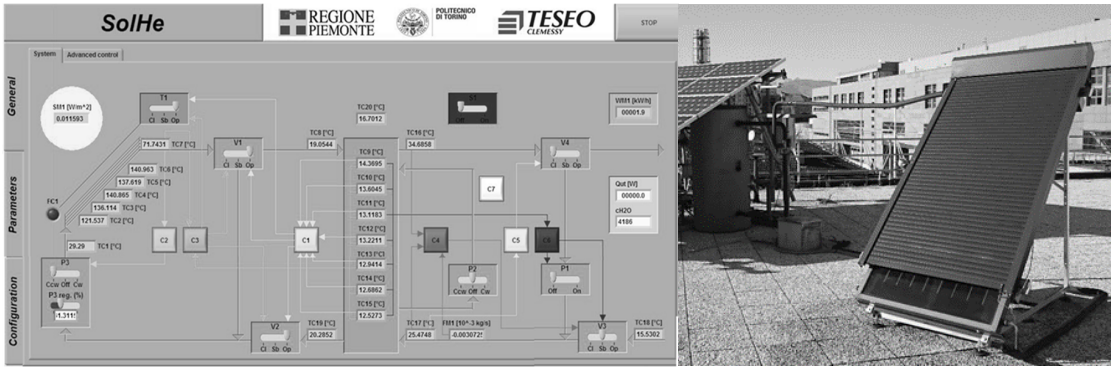

Fig. 3: Left: schematic of the analysed PCS-based solar thermal system. Right: the full scale prototype at Politecnico di Torino.

Figure 3(left) reports a schematic of the prototype and its monitoring system, while Figure 3(right) is a picture of the real scale system installed on the roof of the energy laboratories of Politecnico di Torino. The main component was the solar thermal collector with a net area of 2.1 m^2. The panel was equipped with a motorised cover that worked both as a protection for adverse weather conditions and as a strategy to avoid an undesired overheating of the HTF. The TES tank volume was equal to 200 l. The TES connected the primary collector loop with the demand side heat exchanger that was an internal copper coil of 2.5 kW. A fiberglass insulation layer of 10 cm limited the TES thermal losses to the external ambient. Moreover 8 visors were installed in the TES to visually evaluate the fluid inside the tank. To move the PCS without damaging the PCM micro-capsules dispersed in the mixture, two peristaltic pumps were used, one for the primary collector loop and one in the TES to continuously recirculate the fluid and thus limit the creaming phenomenon (Fan et al., 2015). The peristaltic pump in the primary collector loop was the one controlled by means of the PID controller. Four

solenoid valves were used to control the RBC logics and the operating modes of the solar thermal system (Serale et al., 2015).

4. Experimental tests undertaken to derive the PCS features

The PCS used as HTF was a mixture of water with glycol and a dispersed micro-encapsulated PCM. The PCM contained in the micro-capsules core selected for this application was n-eicosane with a nominal melting temperature of about 36 °C and a specific enthalpy of fusion equal to 195 kJ/kg. Since the thermal properties of the whole PCS mixture strongly depended on the capsule concentrations experimental tests were necessary to define the enthalpy or specific heat vs. temperature curves. The T-History method was selected as the most suitable experimental test for this approach. T-History method defines the correlation between the fluid temperature and its enthalpy at the various micro-encapsulated PCM concentrations. In this case the concentration suitable for the adoption in the solar thermal system were investigated. An extensive description of the T-History tests for the analysed PCS can be find in (Buttitta et al., 2015).
Elaborating the monitored data of the T-history method experiments it was possible to find the enthalpy vs temperature curves at different concentrations using the correlations of Marvin et al. (Marin et al., 2003) (eq. 5-7).

$$H_m = \frac{m_w c_{p,w} + m_t c_{p,t}}{m_t} \frac{A_2}{A_1'} (T_0 - T_s) \qquad \text{(eq.5)}$$

$$\Delta H_p(T_i) = \left(\frac{m_w c_{p,w} + m_t c_{p,t}}{m_p}\right) \frac{A_i}{A_i'} \Delta T_i - \frac{m_t}{m_p} c_{p,t}(T_i) \Delta T_i \qquad \text{(eq.6)}$$

$$H_p(T) = \sum_{i=1}^{n} \Delta H_{p,i} + H_{p,r} \qquad \text{(eq.7)}$$

where H_m is the latent heat, H_p is the enthalpy of the micro-capsule of PCM, $H_{p,r}$ is the enthalpy of a reference fluid whose value is assumed known (in this case distilled water was used as reference fluid), T_0 is the fluid temperature at the experiment initial condition, T_s is the initial temperature of the phase change transition, A_1' is the integral of the temperature difference between the reference fluid and the ambient temperature, A_2 is the integral of the temperature difference between the PCS fluid and the ambient temperature. Both the integrals refer to a period of time ranging from the beginning till the end of the phase change transition. The subscript w indicates the water, whereas t is the tube of the sampler and i is the i-th time instant.
Afterwards, the calculation of the specific heat was possible. The specific heat is defined as the derivative of the enthalpy - temperature curve. The trend of the specific heat can be described as the combination of two Gaussian curves, one for the liquid part and the other one for the solid part (eq. 8).

$$c = \begin{cases} c_s + (c_m - c_s) e^{-\left(\frac{T_m - T}{\omega_s}\right)^2} & T \leq T_m \\ c_l + (c_m - c_l) e^{-\left(\frac{T_m - T}{\omega_l}\right)^2} & T > T_m \end{cases} \qquad \text{(eq.8)}$$

in which the subscribe s refers to the solid state, l to the liquid state and m is the peak value.
Thus, the final equation for the enthalpy curve results in eq. 9.

$$h = \begin{cases} c_s(T - T_{min}) - (c_m - c_s) \frac{\sqrt{\pi}}{2} \omega_s \left[\operatorname{erf}\left(\frac{T_p - T}{\omega_s}\right) - \operatorname{erf}\left(\frac{T_p - T_{min}}{\omega_s}\right)\right] & T \leq T_p \\ c_l T - (c_m - c_l) \frac{\sqrt{\pi}}{2} \omega_l \operatorname{erf}\left(\frac{T_p - T}{\omega_l}\right) + (c_m - c_s) \frac{\sqrt{\pi}}{2} \omega_s \operatorname{erf}\left(\frac{T_p - T_{min}}{\omega_s}\right) - c_s T_{min} + T_p(c_s - c_l) & T > T_p \end{cases}$$

(eq.9)

A possible drawback occurring in test regarding PCS was the so called creaming effect. Indeed, the PCM micro-capsules showed a density that was lower than the one of the water in which they were dispersed. Thus, there was a migration process of the PCM micro-capsules in the upper part of the tubes. To limit the phenomenon during the T-History method, the tubes were placed horizontally and this allowed the results accuracy to be improved up to 18 % compared to the vertical position.
The results of the T-History method are shown in Figure 4. These results were implemented in the Simulink numerical model using Look-up tables. Moreover, Table 1 highlights the available latent heat for each analysed concentration. The creaming effect somehow influenced the reliability of the results and the lower the micro-encapsulated PCM concentration the higher this effect. Indeed, for 5 % w.t. concentration of micro-encapsulated PCM the MAPE was 18 %, while for 15 % w.t. of micro-encapsulated PCM concentration the MAPE decreased to 5 %.

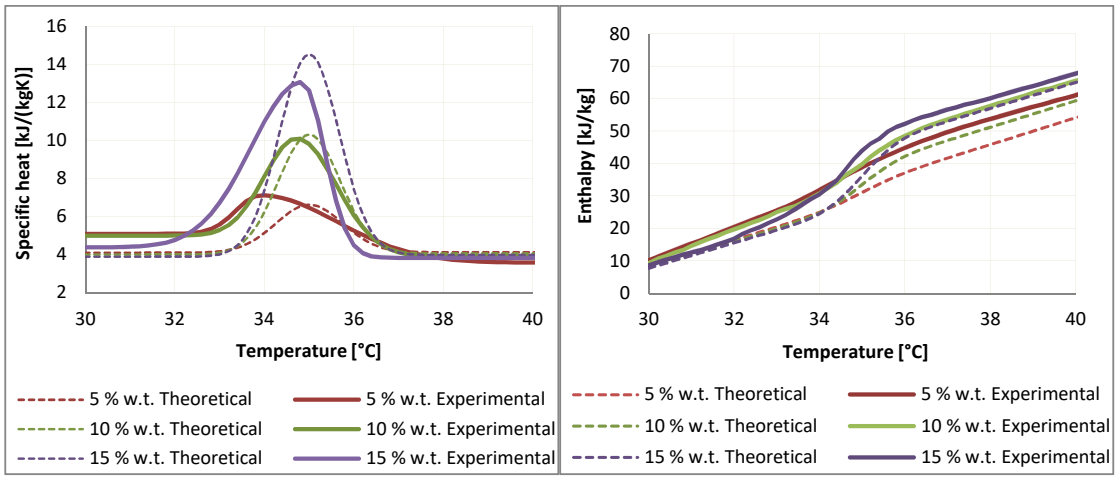

Fig. 4: Left: Enthalpy vs Temperature curves at different weight total concentrations of PCM. Right: Specific heat vs Temperature curve at different weight total concentrations of PCM.

Tab. 1: Comparison between theoretical end experimental PCS latent heat for different concentration of micro-encapsulated PCM in the mixture.

Concentration w.t. [-]	Theoretical latent heat [kJ/kg]	Experimental latent heat [kJ/kg]	MAPE [-]
5 %	4.73	5.74	18 %
10 %	10.97	11.14	2 %
15 %	17.81	18.77	5 %

5. Experimental tests to validate the model

The solar thermal collector and TES prototype were monitored in order to properly identify the parameters of the numerical model that best-fit the actual performance of the prototype. Firstly, the solar thermal collector and the TES were tested as stand-alone elements for 5 days each, afterwards the overall system was monitored for other 5 days. Thus, an uncertainly analysis between the data gathered from the plant and the results obtained from the numerical model has been done.

The implementation of the PID controller in the numerical model allowed not only to perform realistic simulations replicating the real control logics of the prototype, but also to investigate and improve the best Proportional, Integral and Derivative setting. Figure 5(left) shows the comparison of the temperature trend at the outlet of the real collector with the simulated data obtained introducing a P controller and a PI controller. The set-point tracked by the controller was a temperature of 40 °C at the outlet of the solar collector. The P value allowed the set-point temperature to be reached faster, while the I value deleted the error in permanent

regime where the disturbances were constants. The changes in the collector outlet temperature were due to the variation of the flow rate, influenced by controlling the peristaltic pump speed.
On the one hand adopting the P controller, when high level of solar radiation became available, the rotation speed of the pump decreased until the set-point temperature was reached (Figure 5(right)). However, if the solar radiation remained constant, it would not be possible to maintain the 40 °C set point with the P controller and the collector outlet temperature raised up to 44 °C. On the other hand, the combination of a P value with a I value solved this issue. Indeed, it is possible to infer from Figure 5(left) as the set-point was maintained also during all the central hours of sunny days when the solar radiation reached the highest levels. On the contrary, with either P or PI controller during cloudy days (e.g. the fourth and the fifth days of the monitored week), also maintaining the pump speed at the minimum value, the system was not able to reach the set-point could.

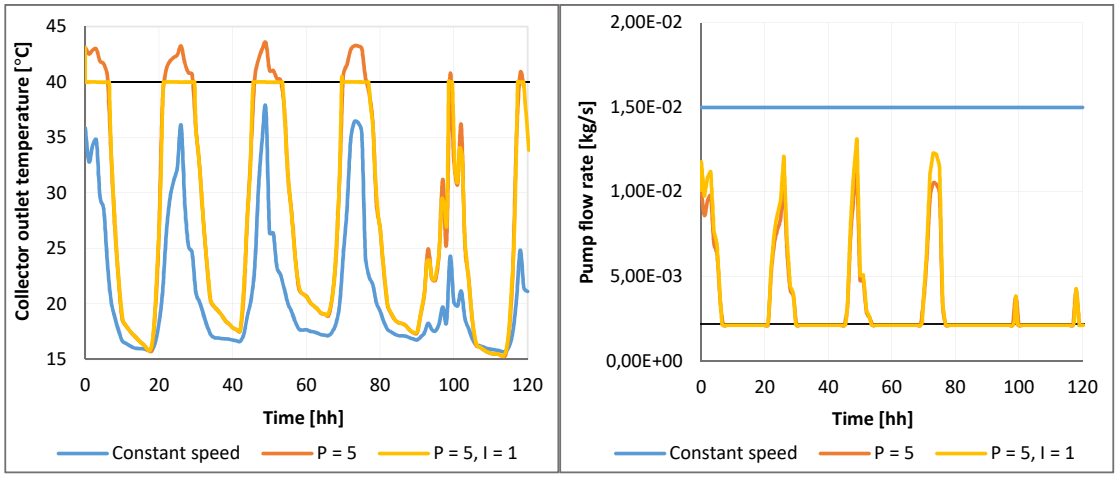

Fig. 5: Experimental results with different combinations of P and PI values. Left: Temperature at the outlet of the collector. Right: HTF pump flow-rates.

At the end of the calibration process for the solar thermal collector, the MAPE between measured and simulated outlet fluid temperatures with water was 1.8 % (i.e., a MAE of 0.5 °C). While the tests of the TES tank temperatures provided a MAPE equal to 1.6 % (i.e., a MAE of 0.3 °C). After those satisfactory results, the analyses of the entire closed loop system were performed. In this case, the difference between the simulated and the monitored data slightly increased. Nevertheless, the error indicators remained smaller than a MAPE of 8 % for the outlet temperature of the solar thermal collector and of 1.8 % for the TES nodes temperatures. The following Figure 6(left) shows the comparison between the simulation and monitored results obtained for the closed loop solar thermal system for 7 monitored temperature in the TES, whereas Figure 6(right) shows the collector outlet temperature.
The simulated trend of the collector outlet temperature followed the experimental results proving a good accuracy. Some small discrepancies were outlined only during peak loads of solar radiation and morning time. This was mainly due a difficult calibration of the solar radiation transmission coefficient of the solar collector glass cover as a function of the incidence angle. Indeed, this transmission coefficient strongly affected the panel performance, influencing the amount of the radiation effectively incident to the absorption plate of the collector. A delay affected the simulated results of the first hours of the day also concerning the TES temperature trends. This was influenced again by the uncertainties affecting the solar collector. Indeed, the outlet of the solar collector was the inlet of the TES.

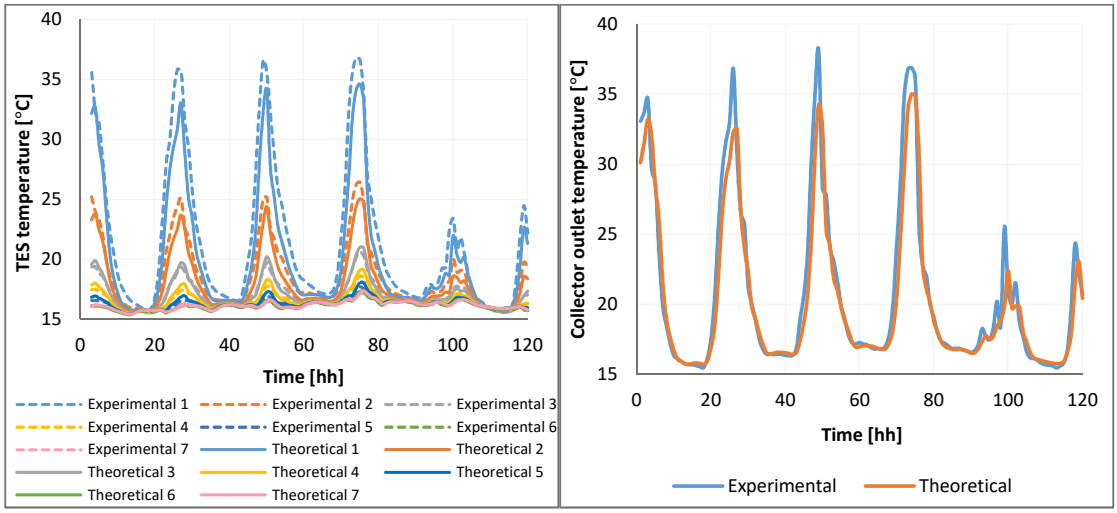

Fig. 6: Experimental vs simulation results. Left: Temperature at the outlet of the collector. Right: Temperatures of the 7 nodes of the TES tank.

The simulated trend of the collector outlet temperature followed the experimental results proving a good accuracy. Some small discrepancies were outlined only during peak loads of solar radiation and morning time. This was mainly due a difficult calibration of the solar radiation transmission coefficient of the solar collector glass cover as a function of the incidence angle. Indeed, this transmission coefficient strongly affected the panel performance, influencing the amount of the radiation effectively incident to the absorption plate of the collector. A delay affected the simulated results of the first hours of the day also concerning the TES temperature trends. This was influenced again by the uncertainties affecting the solar collector. Indeed, the outlet of the solar collector was the inlet of the TES. Eventually, a further discrepancy between real monitored data and simulation results was related to a temperature peak shift in the TES nodes farer from the TES inlet. Simulation results generally anticipated the real monitored data. This was due to some TES internal partitions that slowed down the HTF motion in the real tank and were not modelled in the lumped numerical model.

6. Conclusions

In the present paper a numerical model to describe the physical behaviour and the system dynamics of a complete PCS-based solar thermal system (collector, thermal energy storage and control logics) was presented. The HTF thermal properties were defined by means experimental laboratory tests whose results were herewith reported. Simulation performed by means of the numerical model resulted accurate enough to reproduce the real data gathered in-field during a monitoring campaign on a real scale prototype. Thus, the numerical model can be used in future works to perform comparative analyses to outline the possible benefits achievable by means of the proposed technology. Future works will also deal with additional experimental campaign aiming at adopting as HTF a PCS at different concentrations.

7. References

Buttitta, G., Serale, G., Cascone, Y. 2015. Enthalpy-temperature evaluation of slurry phase change materials with T-history method. Energy Procedia 78, 1877-1882

Cabeza, LF., Ibanez, M., Sole, C., Roca, J., Nogues, M. 2006. Experimentation with a water tank including a PCM module. Solar Energy Materials & Solar Cells 90, 1273–1282

Duffie, J. A., Beckman, W. A. 2013. Solar engineering of thermal processes. John Wiley & Sons.

Eames, PC., Griffiths, PW. 2006. Thermal behaviour of integrated solar collector/storage unit with 65°C phase change material. Energy Conversion and Management 47, 3611–3618

Fan, X., Serale, G., Capozzoli, A., Perino, M. 2015. Experimental measurement and numerical modeling of the creaming of mPCM slurry. Energy Procedia 78, 2010-2015

Haillot, D., Franquet, E., Gibout, S., Bédécarrats, JP. 2013. Optimization of solar DHW system including PCM media. Applied Energy 109, 470–475.

Heier, J., Bales, C., Martin, V. 2015. Combining thermal energy storage with buildings - A review. Renewable and Sustainable Energy Reviews 42, 1305–1325.

Marìn, J., Zalba, B., Cabeza, L. F., Mehling, H. 2003. Determination of enthalpy – temperature curves of phase change materials with the temperature-history method : improvement to temperature dependent. IOP Science, 184.

Pérez-Lombard, L., Ortiz, J., Pout, C. 2008. A review on buildings energy consumption information. Energy and Buildings 40(3), 394–398.

Rodriguez-Ubinas, E., Ruiz-Valero, L., Vega, S., Neila, J. 2012. Applications of Phase Change Material in highly energy-efficient houses. Energy and Buildings 50, 49–62.

Serale, G., Baronetto, S., Goia, F., Perino, M. 2014. Characterization and energy performance of a slurry PCM-based solar thermal collector: A numerical analysis. Energy Procedia 48, 223–232.

Serale, G., Fabrizio, E., Perino, M. 2015. Design of a low-temperature solar heating system based on a slurry Phase Change Material (PCS). Energy and Buildings 106, 44–58.

Serale, G., Goia, F., Perino, M. 2016. Numerical model and simulation of a solar thermal collector with slurry Phase Change Material (PCM) as the heat transfer fluid. Solar Energy 134, 429–444.

Sharma, A., Chen, CR. 2009. Solar Water Heating System with Phase Change Materials. International Review of Chemical Engineering 1, 297–307.

Streicher, W., Bony, J., Citherlet, S., Heinz, A., Pusching, P., Schramzhofer, H., Schultz, J. M. 2008. Simulation models of PCM storage units. A report of IEA solar heating and cooling programme. Task 32, Report C5 of Subtask C. “Advanced storage concepts for solar and low energy buildings”. IEA SHc- Task 32, 1–83.

Various authors, 2012. SHC Annual Report.

IEA-SHC, 2017. URL http://www.iea-shc.org/programme-description (accessed 9.20.17).